



Role of higher-order electric field corrections in the quadrupole interaction of twisted light with matter

ABDULLAH F. ALHARBI^{1,*}  AND ANDREAS LYRAS²

¹King Abdulaziz City for Science and Technology (KACST), P.O. Box 6086, Riyadh 11442, Saudi Arabia

²Quantum Technology Group, Department of Physics and Astronomy, College of Science, King Saud University, Riyadh 11451, Saudi Arabia

*harbi@kacst.edu.sa

Abstract: Recent studies on twisted-light-matter interactions have highlighted the importance of the longitudinal electric field component, which had previously been overlooked. Together with the transverse component, it corresponds to the lowest-order terms in a perturbative expansion over the paraxial parameter. In this work, we investigate the influence of higher-order correction terms in the perturbative expansion on the quadrupole excitation of a trapped atom. This article begins by resolving discrepancies in the literature regarding the calculation of transverse fields at second and higher even orders using the appropriate gauge. A key finding of our study reveals that including a higher-order term in the perturbative expansion is not always sufficient to enhance accuracy in describing the interaction at a given level; instead, two successive orders may need to be considered together. This is particularly evident in quadrupole transitions involving no change in the magnetic quantum number ($\Delta m = 0$), where longitudinal corrections play a more significant role than their transverse counterparts, despite the latter being lower order. This behavior is attributed to the sensitivity of quadrupole interactions to field gradients and the connection between odd- and even-order fields via transverse gradients.

© 2025 Optica Publishing Group under the terms of the [Optica Open Access Publishing Agreement](#)

1. Introduction

In the paraxial approximation of the Helmholtz wave equation, the complex amplitude of the field is represented as a product of a sinusoidal plane wave and a function varying slowly along the propagation direction. The resultant paraxial wave equation for this function is known to effectively describe propagating beams which are not strongly focused. Laguerre Gaussian (LG) beams, which are types of light with twisted (or vortex) phase, are solutions to the paraxial wave equation in cylindrical coordinates [1–4]. These beams can carry Orbital Angular Momentum (OAM) arising from the helical wave front, in addition to Spin Angular Momentum (SAM) arising from circular polarization. The main characteristics of LG beams can be described by two indices: the angular momentum number ℓ and the number of radial nodes p . The rich properties of twisted light connected to its OAM have made it the focus of numerous fundamental and applied studies [5–9].

Applying the paraxial approximation directly to the Helmholtz equation for the electric field results in a solution with a finite transverse profile. However, this paraxial form of the electric field has no vanishing divergence and, in turn, does not satisfy Maxwell equations [10]. In 1975, Lax *et al.* [11] proposed a semi-analytical method to more accurately account for the paraxial solution within the more general framework involving the exact solution of Maxwell equations. Employing a perturbation method, the completely-transverse paraxial solution was shown to be nothing but the zeroth-order solution of the full equation in the paraxial parameter defined as $f = (kw_0)^{-1}$, where k and w_0 are the wave number and the beam waist, respectively. Higher-order corrections beyond the paraxial approximation, which are not necessarily transverse,

are obtainable using two partial differential equations for f small compared to unity. This pioneering work was the foundation for subsequent more detailed analysis, aiming to obtain, for example, higher-order corrections of the Gaussian [12–15] and LG beams [16–19]. There are also other methods to deal with beam propagation beyond the paraxial approximation such as, vector angular-spectrum representation and diffraction integrals [13,17,20]. However, the Lax series expansion provides the means to analytically explore various effects without fully departing from the paraxial framework.

Recent experimental data and theoretical analysis have revealed that considering only the zeroth-order field (the standard paraxial solution) is, in general, inadequate for addressing light properties and its interaction with matter even under paraxial focusing conditions. The first-order electric field correction, which oscillates parallel to the propagation direction, has been shown to induce non-negligible effects [21–30]. The combination of this longitudinal component and the purely transverse paraxial field is regarded as an improved version of the paraxial approximation. The longitudinal component of paraxial optical vortices has a key role, for example, in atomic quadrupole transitions when the two angular momenta are opposite to each other as shown in [27–29] for atoms trapped near the phase singularity, a node on the beam axis. In a recent work [30], we have shown that this is a general property for any paraxial light by deriving analytical formulas for the position-dependent angular-momentum selection rules.

A crucial question now arises regarding the role of higher-order terms in the perturbative expansion, with respect to the paraxial parameter, in twisted light-atom interactions. This work addresses this question by examining the parameters that affect their role in accurately describing atomic quadrupole transitions. Importantly, it demonstrates that advancing to higher orders in the perturbative expansion does not necessarily yield greater accuracy at a certain order of f ; rather, two successive terms in the expansion may need to be considered together. In the first part of this article, we provide a key clarification on the calculation of transverse fields at second and higher even orders in the paraxial parameter, resolving existing discrepancies in the literature. This work lays the theoretical groundwork for understanding higher-order corrections in twisted-light-matter quadrupole interactions, providing a basis for future numerical and experimental investigations.

2. Transition amplitude and the paraxial field

The angular-momentum selection rules for the twisted-light-photoexcitation can be derived using the Power-Zienau-Woolley (PZW) formalism [31–33]. Atomic transitions driven by OAM light are mainly governed by quadrupole interactions [34,35]. The corresponding transition matrix element for a transition from an initial state $|I\rangle$ to a final state $|F\rangle$ is represented in this formalism by:

$$M_{qd} = -\frac{1}{2} \sum_{ij} \langle F | Q_{ij} | I \rangle \nabla_i E_j \quad (1)$$

where $Q_{ij} = e x'_i x'_j$ are the quadrupole transition operators with x'_i the components of the internal position vectors. E_j are the electric field components along x, y and z directions which are going to be derived below.

In order to avoid the inconsistency between the paraxial approximation and Maxwell equations, the Helmholtz wave equation can be first written for the vector potential \mathbf{A} instead of the electric field [2,12]. This will result naturally in the improved paraxial form for the electric field. The suitable gauge for this purpose is the Lorenz gauge where the divergence of \mathbf{A} is nonzero. After applying the paraxial approximation to the equation, one can obtain the following solution for a circularly polarized LG $_{\ell p}$ mode of indices ℓ and p propagating along z :

$$\mathbf{A} = \frac{(\hat{\mathbf{x}} + i\sigma\hat{\mathbf{y}})}{\sqrt{2}} A_0 u_0(\mathbf{r}) e^{(-i\omega t + ikz)} + c.c., \quad (2)$$

where $\sigma=1(-1)$ for left (right) circular polarization, ω is the angular frequency, k is the wavenumber in the longitudinal direction, A_0 is a normalization factor which can be determined by the average power of the beam (the integral of the z -component of the Poynting vector over the beam cross-section) and $u_0(\mathbf{r})$ is the mode function given by:

$$u_0(\mathbf{r}) = \frac{w_0}{w(z)} \left(\frac{\rho}{w(z)} \right)^{|\ell|} L_p^{|\ell|} \left(\frac{2\rho^2}{w_0^2} \right) \times \exp \left(i\ell\varphi - \frac{\rho^2}{w(z)^2} + \frac{ik\rho^2}{2R(z)^2} - i(2p + |\ell| + 1) \arctan\left(\frac{z}{z_R}\right) \right) \tag{3}$$

where ρ is the radial distance from the center axis of the beam, $w(z)$ is the radius at which the field amplitudes fall to $1/e$ of their axial values with $w_0 = w(0)$, $L_p^{|\ell|}(\frac{2\rho^2}{w_0^2})$ is an associated Laguerre polynomial, z_R is the Rayleigh length and $R(z)$ is the radius of curvature of the beam's wavefronts at z , defined as $R(z) = z(1 + \frac{z^2}{z_R^2})$.

Exploiting the Lorenz condition ($\tilde{\nabla} \cdot \mathbf{A} = -\frac{1}{c^2} \frac{\partial \Phi}{\partial t}$), one can obtain the scalar potential Φ . The positive-frequency part of the electric field \mathbf{E} is related to both Φ and \mathbf{A} as follows:

$$\mathbf{E}^{(+)}(\mathbf{r}) = i\omega\mathbf{A} - \frac{\partial \Phi}{\partial z} \hat{\mathbf{z}} - \nabla_{\perp} \Phi \tag{4}$$

where ∇_{\perp} is the transverse gradient. To comprehend the relevance of the different terms in the context of the field corrections, we rewrite expression (4) in terms of the following dimensionless variables:

$$x = w_0\tilde{x}, \quad y = w_0\tilde{y}; \quad z = l\tilde{z} \tag{5}$$

where $l = kw_0^2$ is the diffraction length, so that it can be expressed in powers of f . Consequently, the three terms in the expression for the electric field in (4) corresponds to different orders in f as follows:

$$\mathbf{E}^{(+)}(\mathbf{r}) = (E_{\tilde{x}}^{(0)} \hat{\mathbf{x}} + E_{\tilde{y}}^{(0)} \hat{\mathbf{y}}) + if \left(\frac{\partial E_{\tilde{x}}^{(0)}}{\partial \tilde{x}} + \frac{\partial E_{\tilde{y}}^{(0)}}{\partial \tilde{y}} \right) \hat{\mathbf{z}} + f^2 \tilde{\nabla}_{\perp} \left(\frac{\partial E_{\tilde{x}}^{(0)}}{\partial \tilde{x}} + \frac{\partial E_{\tilde{y}}^{(0)}}{\partial \tilde{y}} \right) \tag{6}$$

where $\tilde{\nabla}_{\perp}$ is the transverse gradient in terms of the dimensionless variables (\tilde{x}, \tilde{y}) . Combining the zeroth- and first-order terms, one can form the expression of the electric field in the improved version of the paraxial approximation:

$$\mathbf{E}^{(+)}(\mathbf{r}) = \mathbf{E}_{\perp}^{(0)} + \mathbf{E}_{\mathbf{z}}^{(1)} \tag{7}$$

On the other hand, the derivatives of the scalar potential with respect to the transverse coordinates lead to transverse terms, which are second-order in f . These terms are considered beyond the validity of the paraxial approximation, as will be clarified below; thus they are routinely neglected [21,36].

3. Corrections to the paraxial approximation

Following the efforts of Lax et al [11] in obtaining corrections to the paraxial solution, Davis [12] has developed a closely related method by first expanding the vector potential as a power series in terms of the paraxial parameter. Then the corrections to the electric field are determined

using the Lorenz gauge, presented in (4). For the sake of simplicity, we limit our discussion in this section to the case of linear polarization. Therefore, the vector potential can be written as:

$$\mathbf{A} = \hat{\mathbf{x}} A_0 u(\mathbf{r}) e^{(-i\omega t + ikz)} + c.c., \quad (8)$$

The general mode function u obeys the Helmholtz wave equation which can be expressed in dimensionless variables as follows:

$$\tilde{\nabla}_{\perp}^2 u + 2i \frac{\partial}{\partial \tilde{z}} u + f^2 \frac{\partial^2}{\partial \tilde{z}^2} u = 0 \quad (9)$$

In the paraxial approximation, the term that scales with f^2 in the full wave equation is disregarded, as presented in expression (7). The perturbative solution of this equation is assumed to be in the form of an infinite power series [12]:

$$u = u^{(0)} + f^2 u^{(2)} + f^4 u^{(4)} + \dots \quad (10)$$

It can be easily verified that $u^{(0)}$, the zeroth order term in f , has to obey the paraxial wave equation leading to the zeroth order vector potential. After applying the Lorenz gauge, one can also obtain the same expressions for $\mathbf{E}_{\perp}^{(0)}$ and $\mathbf{E}_z^{(1)}$ provided in (6). On the other hand, $u^{(2s)}$ ($s = 1, 2, 3, \dots$) has to obey the following differential equation:

$$\tilde{\nabla}_{\perp}^2 u^{(2s)} + 2i \frac{\partial}{\partial \tilde{z}} u^{(2s)} = -\frac{\partial^2}{\partial \tilde{z}^2} u^{(2s-2)} \quad (11)$$

In the case of a complex-argument LG beam, the zeroth-order mode function $\bar{u}_{\ell,p}^{(0)}$ is given by:

$$\bar{u}_{\ell,p}^{(0)} = (-1)^p p! \zeta^{|\ell|+p+1} \tilde{\rho}^{|\ell|} L_p^{|\ell|}(\zeta \tilde{\rho}^2) e^{-\zeta \tilde{\rho}^2} e^{i\ell\varphi} \quad (12)$$

where $\zeta = (1 + 2i\tilde{z})^{-1}$ and $\tilde{\rho} = \rho/w_0$. Takenaka et al [16] solved for $\bar{u}_{\ell,p}^{(2s)}$ analytically obtaining :

$$\bar{u}_{\ell,p}^{(2s)} = \sum_{m=1}^s \frac{(-1)^{s+m}}{s(m-1)!} \binom{2s}{s-m} (1 - \zeta^{-1})^m \bar{u}_{\ell,p+s+m}^{(0)} \quad (13)$$

Employing this result, a recent work obtained the expression of $u_{\ell,p}^{(2s)}$ for a real-argument LG beam to be [19]:

$$u_{\ell,p}^{(2s)} = (-1)^p \sum_{q=0}^p \frac{2^q}{q!} \binom{|\ell|+p}{p-q} \bar{u}_{\ell,q}^{(2s)} \quad (14)$$

Following [12], the authors derived the second-order correction ($s = 1$) for the electric field using the Lorenz gauge [19]:

$$\mathbf{E}_{L,\perp}^{(2)} = i\omega A_0 e^{ikz} f^2 \left(\hat{\mathbf{x}} u_{\ell,p}^{(2)} + \tilde{\nabla}_{\perp} \left(\frac{\partial}{\partial \tilde{x}} u^{(0)} \right) \right) \quad (15)$$

It is interesting to observe that $\mathbf{E}_{L,\perp}^{(2)}$ contains the transverse gradient of the zeroth order field. It is the same part which was ignored in the paraxial expression (6). This term in (15) introduces an additional component to the transverse field along the y-axis. This result contradicts with the correction scheme of Lax and co-authors described in [11,37] which has been derived directly

from Maxwell equations using the electric field. In this scheme, the electric field is expressed in powers of f as follows:

$$\begin{aligned} \mathbf{E}^{(+)}(\mathbf{r}) &= \hat{\mathbf{x}} E_{\perp} + \hat{\mathbf{z}} E_z \\ &= e^{ikl\tilde{z}} \left(\hat{\mathbf{x}} \sum_{s=0}^{\infty} f^{2s} \psi^{(2s)} + \hat{\mathbf{z}} \sum_{s=0}^{\infty} f^{(2s+1)} \psi^{2s+1} \right) \end{aligned} \quad (16)$$

The expansion includes alternate orders, i.e., the transverse (longitudinal) components are expressed as a power series of even (odd) orders of f . The functions $\psi^{(2s)}$, with $s = 1, 2, 3, \dots$, are obtained by solving the same differential Eq. (11) used to find $u^{(2s)}$. So both functions must have the same spatial dependence and to be directly proportional to each other. Moreover, it can be noted that the polarization state of the transverse field in (16) remains intact regardless of the order of the correction, in contrast to expression (15).

It is crucial to examine why the earlier approach, based on the systematic expansion of the vector potential, fails to align with the work of Lax et al. [11] beyond the first-order correction. This disagreement can be traced back to an improper choice of the gauge. While the Lorenz gauge is conventionally used for deriving paraxial beams with Gaussian or Laguerre-Gaussian (LG) radial profiles, it proves inadequate in this context, where the full wave equation is applied and a power-series solution beyond the paraxial approximation is required. Instead, the Coulomb gauge must be employed in this scenario.

Considering that the ansatz for the spatial mode of the zeroth-order field must correspond to the transverse paraxial solution, it can be shown that the electric fields derived from both the Lorenz and Coulomb gauges agree only up to the first order in f . However, gauge-dependent differences arise in all higher-order terms. We emphasize that this result does not contradict the gauge independence of electric and magnetic fields. This is a special case, where the zeroth-order transverse spatial mode of \mathbf{A} is constrained. Under this constraint, it can be shown that no gauge transformation exists to connect the two sets of potentials produced by these gauges [36].

The vector potential in the Coulomb gauge $\mathbf{A}^C(\mathbf{r})$ has non-vanishing longitudinal component in addition to the transverse component. The latter can be expanded in even powers of f as explained in the earlier approach and admits the same solutions. On the other hand, the power-series solution for the longitudinal component is in odd orders of f and is determined by the Coulomb condition:

$$\frac{\partial}{\partial \tilde{z}} A_z^C = f^{-1} \tilde{\nabla}_{\perp} \cdot \mathbf{A}_{\perp}^C \quad (17)$$

In the Coulomb gauge, the vector potential is related to the electric field as follows:

$$\mathbf{E}^{(+)}(\mathbf{r}) = i\omega \mathbf{A}^C(\mathbf{r}) \quad (18)$$

This leads to the following expression for $E_{\perp}^{(2)}$:

$$\mathbf{E}_{\perp}^{(2)} = \hat{\mathbf{x}} i\omega A_0 e^{ikl\tilde{z}} f^{(2)} u_{\ell,p}^{(2)} \quad (19)$$

Using this expression with $\ell = p = 0$, one can recover the form of the second order correction for the fundamental Gaussian beam, as derived by Agrawal et al. in [13].

To highlight the differences between the two expressions given in (15) and (19), we set $p = 0$, as it is experimentally widely used and assume that the focal plane is shifted from the $\tilde{z} = 0$ plane to a parallel plane at $\tilde{z} = z_0 > 0$, so that $w_0 = w(\tilde{z} - z_0)$. The expression (19), therefore, reads:

$$\mathbf{E}_{\perp}^{(2)} = \hat{\mathbf{x}} 2\tilde{z}\omega A_0 e^{ikl(\tilde{z}-z_0)} f^{(2)} \bar{u}_{\ell,2}^{(0)} \quad (20)$$

On the other hand, the expression (15) is equal to (19) plus additional terms, so for this case, it takes the following form:

$$\begin{aligned} \mathbf{E}_{L,\perp}^{(2)} = & \mathbf{E}_{\perp}^{(2)} + i\omega A_0 e^{ikl(\tilde{z}-z_0)} f^{(2)} u_{\ell,0}^{(0)} \\ & \times \left\{ \hat{\mathbf{x}} \left(\left(\frac{|\ell|}{\tilde{\rho}} e^{-i\gamma\varphi} - 2\tilde{\rho} \cos \varphi \right)^2 - \frac{|\ell|}{\tilde{\rho}^2} e^{-2i\gamma\varphi} - 2 \right) \right. \\ & \left. + \hat{\mathbf{y}} \left(\left(\frac{\ell}{\tilde{\rho}} e^{-i\gamma\varphi} - 2\tilde{\rho} \sin \varphi \right) \left(\frac{|\ell|}{\tilde{\rho}} e^{-i\gamma\varphi} - 2\tilde{\rho} \cos \varphi \right) - i \frac{|\ell|}{\tilde{\rho}^2} e^{-2i\gamma\varphi} \right) \right\} \end{aligned} \quad (21)$$

where $\gamma = \frac{\ell}{|\ell|}$. It should be noted that the amplitude of the second-order field correction derived using the Coulomb gauge ($\mathbf{E}_{\perp}^{(2)}$) is fundamentally different from the corresponding result obtained using the Lorenz gauge ($\mathbf{E}_{L,\perp}^{(2)}$). This distinction lies not only in the magnitude of the field along the x-axis but also in its vector form through the presence of an additional y-component. Notably, there are cases where one of the field forms vanishes while the other does not. For example, $\mathbf{E}_{\perp}^{(2)}$ is always zero around the phase singularity regardless of the value of ℓ . On the other hand, $\mathbf{E}_{L,\perp}^{(2)}$ is nonzero in this region for $|\ell| = 2$ due to the presence of ρ^2 in the denominator. This may lead to incorrect prediction for certain phenomena. In particular, for atomic quadrupole transitions induced by LG beam with $\ell = -2\sigma$, considering the second order correction to the field in the misleading form of (21) doubles the strength of $\Delta m = \pm 1$ transitions, reported in [30]. Moreover, $\mathbf{E}_{\perp}^{(2)}$ depends linearly on the longitudinal distance from the $\tilde{z} = 0$ plane, so it vanishes as $\tilde{z} \rightarrow 0$. In contrast, the additional terms in $\mathbf{E}_{L,\perp}^{(2)}$ exhibit no such dependence. As a result, the comparison between the two approaches is not merely a matter of quantitative difference but rather of fundamental qualitative difference that when considered in the context of the Lax et al correction scheme [11], becomes a conceptual difference.

The third-order correction, in terms of the lower-order terms, can be determined to be:

$$\mathbf{E}_{\tilde{z}}^{(3)} = \hat{\mathbf{z}} i e^{ikl(\tilde{z}-z_0)} f^3 (\nabla_{\perp} \cdot \mathbf{F}_{\perp}^{(2)} + \frac{\partial}{\partial \tilde{z}} F_{\tilde{z}}^{(1)}) \quad (22)$$

where we define $\mathbf{E}^{(+)}(\mathbf{r}) = e^{ikl(\tilde{z}-z_0)} (\mathbf{F}_{\perp} + F_{\tilde{z}} \hat{\mathbf{z}})$. This relation is also true for any higher odd-order correction and it agrees with the results of Lax's scheme [11].

4. Quadrupole transitions

This section investigates the influence of higher-order electric field corrections on twisted light-matter interactions, with a focus on quadrupole transitions. A major aim is to examine if the significant contribution of the longitudinal field components relative to the transverse ones reported in the literature [27,30], as explained in Fig. 1, persists at higher orders. We restrict our discussion to electric field corrections up to the third order, as they represent the leading terms. Most of the results presented here can be generalized to higher-order corrections. The connection between odd- and even-order fields can be summarized in the following expressions:

$$\begin{aligned} F_{\tilde{z}}^{(1)} &= i \tilde{\nabla}_{\perp} \cdot \mathbf{F}^{(0)} \\ F_{\tilde{z}}^{(3)} &= i \tilde{\nabla}_{\perp} \cdot \mathbf{F}_{\perp}^{(2)} + i \frac{\partial}{\partial \tilde{z}} F_{\tilde{z}}^{(1)} \end{aligned} \quad (23)$$

The longitudinal gradient of $F_{\tilde{z}}^{(1)}$ can be ignored near the center of the beam at the beam focus in the range where the diffraction length is larger than the wavelength of the light [36]. Restricting

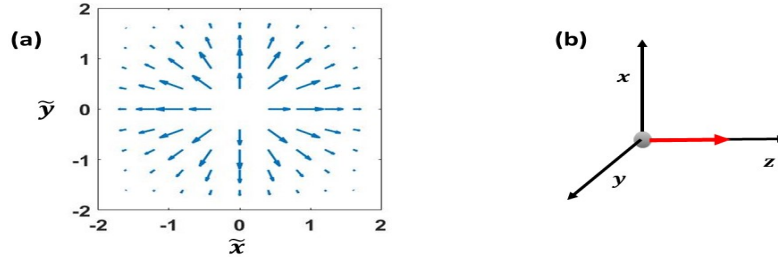


Fig. 1. (a) Transverse cut of Laguerre-Gaussian beam with antiparallel spin and orbital angular momenta ($\ell = -\sigma$). The arrows represent the magnitude and direction of the paraxial transverse field component across the plane of the dimensionless coordinates (\tilde{x}, \tilde{y}) . (b) Schematic of the polarization vector of the electric field at the center of the focused beam where a trapped atom is located. Although the transverse component near the phase singularity vanishes, the non-zero transverse gradient of its field induces atomic quadrupole transitions with $\Delta m = 0$. On the other hand, the longitudinal component, which is also proportional to the transverse gradient of the transverse component, exhibits a Gaussian form that peaks at the center. $\Delta m = 0$ quadrupole excitation from the longitudinal component depends on its longitudinal gradient. These effects make the contribution of the longitudinal component relatively more significant for this particular transition.

the treatment to this region, we can rewrite the above equations in the following compact form:

$$F_z^{(2n+1)} = i \tilde{\nabla}_\perp \cdot \mathbf{F}_\perp^{(2n)} \quad (24)$$

where $n=0,1$. Since the matrix element (1) contains derivatives of the field, the order of terms involving the longitudinal gradient of the $(2n+1)^{th}$ -order field correction is reduced, so that they become comparable to terms involving the transverse gradient of the $(2n)^{th}$ -order correction. Moreover, the relationships between the quadrupole operators may amplify the contribution of the higher order field, as shown below.

Employing expression (1), one can show that there are two channels for an atomic quadrupole transition with magnetic quantum number difference $\Delta m = 0$ induced by an LG beam with $\ell = -\sigma$:

- 1 Channel M_\perp associated with the transverse gradient of the fields $E_{\tilde{x},\tilde{y}}^{(2n)}$. M_\perp is given by:

$$\begin{aligned} M_\perp^{(2n)} &= -\frac{1}{2w_0} \left(\langle Q_{xx} \rangle \frac{\partial E_{\tilde{x}}^{(2n)}}{\partial \tilde{x}} + \langle Q_{yy} \rangle \frac{\partial E_{\tilde{y}}^{(2n)}}{\partial \tilde{y}} \right) \\ &= -\frac{1}{2w_0} \langle Q_{xx} \rangle \left(\frac{\partial E_{\tilde{x}}^{(2n)}}{\partial \tilde{x}} + \frac{\partial E_{\tilde{y}}^{(2n)}}{\partial \tilde{y}} \right) \end{aligned} \quad (25)$$

Here we used the result $\langle Q_{xx} \rangle = \langle Q_{yy} \rangle$.

- 2 Channel M_z associated with the longitudinal gradient of the field $E_z^{(2n+1)}$. The corresponding quadrupole transition operator is Q_{zz} , where $\langle Q_{zz} \rangle = -2 \langle Q_{xx} \rangle$. So we can write:

$$\begin{aligned} M_z^{(2n+1)} &= -\frac{1}{2l} \langle Q_{zz} \rangle \frac{\partial E_z^{(2n+1)}}{\partial \tilde{z}} \\ &= -kf \langle Q_{xx} \rangle \left(\frac{\partial E_{\tilde{x}}^{(2n)}}{\partial \tilde{x}} + \frac{\partial E_{\tilde{y}}^{(2n)}}{\partial \tilde{y}} \right) \\ &= 2M_\perp^{(2n)} \end{aligned} \quad (26)$$

The finding that that $M_z^{(2n+1)}$ is larger than $M_\perp^{(2n)}$ for $n = 0$ and 1 , respectively, originates from two primary factors. First, an odd-order correction arises from the transverse gradient of the preceding even-order term in the expansion. Second, $M_\perp^{(2n)}$ ($M_z^{(2n+1)}$) is proportional to the transverse (longitudinal) gradient of the even-order (odd-order) field. Consequently, the order of the transition amplitude $M_z^{(2n+1)}$ in f is reduced by one order to match that of $M_\perp^{(2n)}$. The factor of two in the ratio of M_z to M_\perp emerges from the relationships among the involved expectations values of the quadrupole transition operators.

Having examined the role of longitudinal corrections in quadrupole transitions compared to transverse corrections, it is also important to consider the influence of the second- and third-order corrections relative to the lowest ones. The ratio of matrix elements $M_\perp^{(2)}$ to $M_\perp^{(0)}$ is governed by the transverse gradient of the transverse fields $\mathbf{E}_\perp^{(2)}$ and $\mathbf{E}_\perp^{(0)}$. This ratio is particularly interesting when calculated at the focus in the region near the phase singularity [27], where quadrupole transitions induced by LG beams with $|\ell| = 1$ are nonzero only for $\ell = -\sigma$. In this case, the mode functions $u_{10}^{(2)}$ and $u_{10}^{(0)}$ are related as follows:

$$u_{10}^{(2)} = -12 i z_0 u_{10}^{(0)} \tag{27}$$

Thus, the ratio of matrix elements reads:

$$\left| \frac{M_\perp^{(2)}}{M_\perp^{(0)}} \right| = 12 f^2 z_0 \tag{28}$$

We observe that the importance of the correction in quadrupole excitation depends on the degree of focusing through both the square of the paraxial parameter and the scaled propagation distance along the z -axis, measured from the $z=0$ plane, where the field is assumed to be fully paraxial.

It is evident from (27) that the second-order field correction near the phase singularity follows the same radial profile as the zeroth-order field. At paraxial focusing conditions ($f \ll 1$), the contribution of $E^{(2)}$ is therefore overwhelmed by the dominant contribution of $E^{(0)}$. As the trapped atom moves laterally away from the center, the spatial structure of higher-order corrections diverges from that of the lowest-order fields, leading to variations in their relative contributions to the atomic quadrupole excitation. These radial spatial differences are primarily encoded in the differing degrees of the involved associated Laguerre polynomials. Under tight focusing, the effects of higher-order corrections is more pronounced. Additionally, the overlooked longitudinal gradients involved in the definitions of the field corrections and the Hamiltonian need to be considered in this regime.

In contrast to $\Delta m = 0$ transitions, quadrupole $\Delta m = \pm 1$ transitions induced by $E_\perp^{(2)}$ partially depend linearly on the propagation distance. The matrix element for this transition is proportional to the longitudinal derivative of $E_\perp^{(2)}$, which is composed of three terms:

$$\frac{\partial E_\perp^{(2)}}{\partial \tilde{z}} \propto e^{ikl(\tilde{z}-z_0)} \left((ikl) \tilde{z} \bar{u}_{\ell,p}^{(2)} + \tilde{z} \frac{\partial \bar{u}_{\ell,p}^{(2)}}{\partial \tilde{z}} + \bar{u}_{\ell,p}^{(2)} \right) \tag{29}$$

It can be noted that the last term has no linear dependence on the distance from the $z=0$ plane.

A key point to consider is that all odd-order corrections have no contribution to transitions with $\Delta m = \pm 2$. As explained in [30] for the first-order correction, the absence of the longitudinal field channels is attributed to the tensor structure of the quadrupole operator Q_{iz} , where $i = x, y$ or z .

5. Conclusion

The perturbative approach bridges the gap between the standard paraxial approximation and the fully nonparaxial regime. Despite the perturbative expansion was proposed in the mid-1970s,

discrepancies remain in the literature regarding the calculation of transverse fields at second and higher even orders in the paraxial parameter. This work began by resolving these discrepancies through the adoption of a gauge framework consistent with Lax's correction scheme.

We also have demonstrated that the longitudinal corrections play a more significant role for certain quadrupole transitions in a localized atom compared to their transverse counterparts, although the latter are lower by one order in the paraxial parameter. This observation is not solely determined by the degree of focusing. Instead, it also arises from two additional factors: i) a longitudinal correction emerges as the transverse gradients of the preceding transverse correction, and ii) quadrupole transitions are sensitive to electric field gradients. Although this article focused on LG beams, the formalism is general, and the findings are relevant for other types of focused light beams that can be described using the Lax series expansion. Incorporating higher-order corrections allows for more accurate modeling of atomic transitions, enhancing the accuracy of spectroscopic measurements and precise control of twisted-light-matter coupling in quantum information applications, especially for tightly focused beams in the range where the perturbative expansion remains valid.

Funding. King Abdulaziz City for Science and Technology (NSTIP 2-17-01-001-0057).

Acknowledgement. The project was funded by the National Science, Technology and Innovation Plan (NSTIP), King Abdulaziz City for Science and Technology, Kingdom of Saudi Arabia, Award number (2-17-01-001-0057).

Disclosures. The authors declare no competing interests.

Data availability. Data underlying the results presented in this paper are not publicly available at this time but may be obtained from the authors upon reasonable request.

References

1. L. Allen, M. W. Beijersbergen, R. J. C. Spreeuw, *et al.*, "Orbital angular momentum of light and the transformation of Laguerre-Gaussian laser modes," *Phys. Rev. A* **45**(11), 8185–8189 (1992).
2. D. L. Andrews and M. Babiker, *The Angular Momentum of Light* (Cambridge University Press, 2012).
3. S. M. Barnett, L. Allen, R. P. Cameron, *et al.*, "On the natures of the spin and orbital parts of optical angular momentum," *J. Opt.* **18**(6), 064004 (2016).
4. S. M. Barnett, M. Babiker, and M. J. Padgett, "Optical orbital angular momentum," *Phil. Trans. R. Soc. A.* **375**(2087), 20150444 (2017).
5. S. Franke-Arnold, "30 years of orbital angular momentum of light," *Nat. Rev. Phys.* **4**(6), 361 (2022).
6. L. A. Rusch, M. Rad, K. Allahverdyan, *et al.*, "Carrying data on the orbital angular momentum of light," *IEEE Commun. Mag.* **56**(2), 219–224 (2018).
7. M. Krenn, J. Handsteiner, M. Fink, *et al.*, "Twisted light transmission over 143 km," *Proc. Natl. Acad. Sci.* **113**(48), 13648–13653 (2016).
8. M. J. Padgett, "Orbital angular momentum 25 years on," *Opt. Express* **25**(10), 11265–11274 (2017).
9. G. F. Quinteiro, A. O. Lucero, and P. I. Tamborenea, "Electronic transitions in quantum dots and rings induced by inhomogeneous off-centered light beams," *arXiv* (2013).
10. A. Carnicer, I. Juvells, D. Maluenda, *et al.*, "On the longitudinal component of paraxial fields," *Eur. J. Phys.* **33**(5), 1235–1247 (2012).
11. M. Lax, W. H. Louisell, and W. B. McKnight, "From maxwell to paraxial wave optics," *Phys. Rev. A* **11**(4), 1365–1370 (1975).
12. L. W. Davis, "Theory of electromagnetic beams," *Phys. Rev. A* **19**(3), 1177–1179 (1979).
13. G. P. Agrawal and D. N. Pattanayak, "Gaussian beam propagation beyond the paraxial approximation," *J. Opt. Soc. Am.* **69**(4), 575–578 (1979).
14. M. Couture and P.-A. Belanger, "From gaussian beam to complex-source-point spherical wave," *Phys. Rev. A* **24**(1), 355–359 (1981).
15. P. González de Alaiza Martínez, G. Duchateau, B. Chimier, *et al.*, "Maxwell-consistent, symmetry- and energy-preserving solutions for ultrashort-laser-pulse propagation beyond the paraxial approximation," *Phys. Rev. A* **98**(4), 043849 (2018).
16. T. Takenaka, M. Yokota, and O. Fukumitsu, "Propagation of light beams beyond the paraxial approximation," *J. Opt. Soc. Am. A* **2**(6), 826–829 (1985).
17. H. C. Kim and Y. H. Lee, "Hermite-gaussian and laguerre-gaussian beams beyond the paraxial approximation," *Opt. Commun.* **169**(1-6), 9–16 (1999).
18. K. Duan, B. Lü, and B. Wang, "Propagation of Hermite-Gaussian and Laguerre-Gaussian beams beyond the paraxial approximation," *J. Opt. Soc. Am. A* **22**(9), 1976–1980 (2005).

19. I. A. Vovk, N. V. Tepliakov, M. Y. Leonov, *et al.*, “Analytical theory of real-argument Laguerre-Gaussian beams beyond the paraxial approximation,” *J. Opt. Soc. Am. A* **34**(10), 1940 (2017).
20. P. Liu and B. Lü, “The vectorial angular-spectrum representation and rayleigh–sommerfeld diffraction formulae,” *Opt. Laser Technol.* **39**(4), 741–744 (2007).
21. K. A. Forbes, D. Green, and G. A. Jones, “Relevance of longitudinal fields of paraxial optical vortices,” *J. Opt.* **23**(7), 075401 (2021).
22. K. Y. Bliokh and F. Nori, “Transverse and longitudinal angular momenta of light,” *Phys. Rep.* **592**, 1–38 (2015).
23. K. Koksai, M. Babiker, V. E. Lembessis, *et al.*, “Truncated optical Bessel modes,” *Phys. Rev. A* **105**(6), 063512 (2022).
24. A. Aiello, P. Banzer, M. Neugebauer, *et al.*, “From transverse angular momentum to photonic wheels,” *Nat. Photonics* **9**(12), 789–795 (2015).
25. V. E. Lembessis, A. Lyras, and O. M. Aldossary, “Two-level atom dynamics induced by a spin-orbit coupled optical vortex: dressed states formulation,” *Opt. Continuum* **2**(5), 1256–1266 (2023).
26. V. E. Lembessis, K. Koksai, J. Yuan, *et al.*, “Chirality-enabled optical dipole potential energy for two-level atoms,” *Phys. Rev. A* **103**(1), 013106 (2021).
27. G. F. Quinteiro, F. Schmidt-Kaler, and C. T. Schmiegelow, “Twisted-light–ion interaction: The role of longitudinal fields,” *Phys. Rev. Lett.* **119**(25), 253203 (2017).
28. G. F. Q. Rosen, “On the importance of the longitudinal component of paraxial optical vortices in the interaction with atoms,” *J. Opt. Soc. Am. B* **40**(4), C73–C77 (2023).
29. M. Verde, C. T. Schmiegelow, U. Poschinger, *et al.*, “Trapped atoms in spatially-structured vector light fields,” *Sci. Rep.* **13**(1), 21283 (2023).
30. A. F. Alharbi, A. Lyras, and V. E. Lembessis, “Significance of the longitudinal component of paraxial light in position-dependent selection rules for quadrupole atomic transitions,” *Opt. Express* **31**(26), 43690–43697 (2023).
31. E. A. Power and S. Zienau, “Coulomb Gauge in Non-Relativistic Quantum Electro-Dynamics and the Shape of Spectral Lines,” *Phil. Trans. R. Soc. Lond. A* **251**(999), 427–454 (1959).
32. R. G. Woolley, “Molecular Quantum Electrodynamics,” *Proceedings of the Royal Society of London Series A* **321**, 557–572 (1971).
33. V. E. Lembessis and M. Babiker, “Enhanced quadrupole effects for atoms in optical vortices,” *Phys. Rev. Lett.* **110**(8), 083002 (2013).
34. M. Babiker, C. R. Bennett, D. L. Andrews, *et al.*, “Orbital angular momentum exchange in the interaction of twisted light with molecules,” *Phys. Rev. Lett.* **89**(14), 143601 (2002).
35. C. T. Schmiegelow and F. Schmidt-Kaler, “Light with orbital angular momentum interacting with trapped ions,” *Eur. Phys. J. D* **66**(6), 157 (2012).
36. G. F. Quinteiro, C. T. Schmiegelow, D. E. Reiter, *et al.*, “Reexamination of bessel beams: A generalized scheme to derive optical vortices,” *Phys. Rev. A* **99**(2), 023845 (2019).
37. G. P. Agrawal and M. Lax, “Free-space wave propagation beyond the paraxial approximation,” *Phys. Rev. A* **27**(3), 1693–1695 (1983).